N O T I C E

THIS DOCUMENT HAS BEEN REPRODUCED FROM
MICROFICHE. ALTHOUGH IT IS RECOGNIZED THAT
CERTAIN PORTIONS ARE ILLEGIBLE, IT IS BEING RELEASED
IN THE INTEREST OF MAKING AVAILABLE AS MUCH
INFORMATION AS POSSIBLE

STRESSES AND DEFORMATIONS IN ELLIPTICAL CONTACTS

Bernard J. Hamrock
Lewis Research Center
Cleveland, Ohio

NASA

STRESSES AND DEFORMATIONS IN ELLIPTICAL CONTACTS

Bernard J. Hamrock

National Aeronautics and Space Administration
Lewis Research Center
Cleveland, Ohio 44135

CONFORMAL AND NONCONFORMAL SURFACES

Hydrodynamic lubrication is generally characterized by surfaces that are conformal. That is, the surfaces fit snugly into each other with a high degree of geometrical conformity, so that the load is carried over a relatively large area. Furthermore the load-carrying surface area remains essentially constant while the load is increased. Fluid-film journal and slider bearings are conformal surfaces. In journal bearings the radial clearance between the shaft and the bearing is typically one-thousandth of the shaft diameter; in slider bearings the inclination of the bearing surface to the runner is typically one part in a thousand.

Many machine elements have contacting surfaces that do not conform to each other very well. The full burden of the load must then be carried by a very small contact area. In general the contact areas between nonconformal surfaces enlarge considerably with increasing load but are still small compared with the contact areas between conformal surfaces. Some examples of these nonconformal surfaces are mating gear teeth, cams and followers, and rolling-element bearings.

The load per unit area in conformal bearings is relatively low, typically only 1400 N/m² and seldom over 35 000 N/m². By contrast, the load per unit area in nonconformal contacts, such as those that exist in ball bearings, will generally exceed 700 000 N/m², even at modest applied loads. These high pressures result in elastic deformation of materials such that the elliptical contact areas are formed for oil film generation and load support. The significance of the high contact pressures is that they result in a considerable increase in fluid viscosity. Inasmuch as viscosity is a measure of a fluid's resistance to flow, this increase greatly enhances the lubricant's ability to support load without being squeezed out of the contact zone.

Figure 1 shows the nonconformal surfaces of a ball bearing. The ball and race conform to some degree in the section shown in figure 1(a), but the section view shown in figure 1(b) clearly exhibits little conformity. We are concerned only with nonconformal contacts.

CURVATURE SUM AND DIFFERENCE

The undeformed geometry of contacting solids can be represented in general terms by two ellipsoids. The two solids with different radii of curvature in a pair of principal planes (x and y) passing through the contact between the solids make contact at a single point under the condition of zero applied load. Such a condition is called point contact and is shown in figure 2, where the radii of curvature are denoted by r's. It is assumed throughout the lecture that convex surfaces, as shown in figure 2, exhibit positive curvature and concave surfaces, negative curvature. Therefore, if the center of curvature lies within the solid, the radius of curvature is positive; if the center of curvature lies outside the solid, the radius of curvature is negative. It is important to note that if coordinates x and y are chosen such that

$$\frac{1}{r_{ax}} + \frac{1}{r_{bx}} > \frac{1}{r_{ay}} + \frac{1}{r_{by}} \tag{1}$$

coordinate x then determines the direction of the semiminor axis of the contact area when a load is applied and y, the direction of the semimajor axis.

The example of a ball bearing is used to illustrate the definition of the radii of curvature. A cross section of a thrust-loaded ball bearing operating at a contact angle β is shown in figure 3. Equivalent radii of curvature for both inner- and outer-race contacts in, and normal to, the direction of rolling can be calculated from this figure. The radii of curvature for the ball - inner-race contact are

$$r_{ax} = r_{ay} = \frac{d}{2} \tag{2}$$

$$r_{bx} = \frac{d_e - d \cos \beta}{2 \cos \beta} \tag{3}$$

$$r_{by} = -r_i \tag{4}$$

The radii of curvature for the ball - outer-race contact are

$$r_{ax} = r_{ay} = \frac{d}{2} \tag{5}$$

$$r_{bx} = - \frac{d_e + d \cos \beta}{2 \cos \beta} \tag{6}$$

$$r_{by} = -r_o \tag{7}$$

Note that the ball - inner-race and ball - outer-race contact inequality (1) is satisfied and that the sign convention mentioned earlier has been adopted.

The curvature sum and difference, which are quantities of some importance in the analysis of contact stresses and deformations, are

2

$$\frac{1}{R} = \frac{1}{R_x} + \frac{1}{R_y} \tag{8}$$

$$\Gamma = R\left(\frac{1}{R_x} - \frac{1}{R_y}\right) \tag{9}$$

where

$$\frac{1}{R_x} = \frac{1}{r_{ax}} + \frac{1}{r_{bx}} \tag{10}$$

$$\frac{1}{R_y} = \frac{1}{r_{ay}} + \frac{1}{r_{by}} \tag{11}$$

Equations (10) and (11) effectively redefine the problem of two ellipsoidal solids approaching one another in terms of an equivalent ellipsoidal solid of radii R_x and R_y approaching a plane in the manner shown in figure 4. From the radius-of-curvature expressions, the radii R_x and R_y for the contact example discussed earlier can be written for the <u>ball - inner-race contact</u> as

$$R_x = \frac{d(d_e - d\cos\beta)}{2d_e} \tag{12}$$

$$R_y = \frac{r_i d}{2r_i - d} \tag{13}$$

and for the <u>ball - outer-race contact</u> as

$$R_x = \frac{d(d_e + d\cos\beta)}{2d_e} \tag{14}$$

$$R_y = \frac{r_o d}{2r_o - d} \tag{15}$$

GEOMETRICAL SEPARATION OF ELLIPSOIDAL SOLIDS

The geometrical separation $(S_{ax} + S_{bx})$ or $(S_{ay} + S_{by})$ between two ellipsoidal solids is thus made equivalent to that between a single ellipsoidal solid and a plane in the manner shown in figure 4. The geometrical requirement is simply that at any value of x and y (fig. 4(a)) the geometrical separation between the two ellipsoids must be the same as the separation between the equivalent ellipsoid and a plane at the same values of x and y (fig. 4(b)). From figure 4(a) the following can be written:

3

$$r_{ax}^2 = x^2 + (r_{ax} - S_{ax})^2 \tag{16}$$

or

$$x^2 = S_{ax}(2r_{ax} - S_{ax}) \tag{17}$$

But $2r_{ax} \gg S_{ax}$, so (17) becomes

$$S_{ax} = \frac{x^2}{2r_{ax}} \tag{18}$$

This is the well-known parabolic approximation to the circular section of the solid and is valid as long as the separation is much smaller than the radius of curvature. Similar expressions for S_{ay}, S_{bx}, and S_{by} can be written, and the expression for the total separation of an ellipsoidal solid and a plane (fig. 4(b)) can thus be written as

$$S = \frac{x^2}{2R_x} + \frac{y^2}{2R_y} \tag{19}$$

SURFACE STRESSES AND DEFORMATIONS

When an elastic solid is subjected to a load, stresses are produced that increase as the load is increased. These stresses are associated with deformations, which are defined by strains. Unique relationships exist between stresses and their corresponding strains. For elastic solids the stresses are linearly related to the strains, with the constant of proportionality being an elastic constant that adopts different values for different materials. Thus a simple tensile load applied to a bar produces a stress σ_1 and a strain ε_1, where

$$\sigma_1 = \frac{\text{Load}}{\text{Cross-sectional area}} = \text{Stress in axial direction} \tag{20}$$

$$\varepsilon_1 = \frac{\text{Change in length}}{\text{Original length}} = \text{Strain in axial direction} \tag{21}$$

and

$$E = \frac{\sigma_1}{\varepsilon_1} = \text{Elastic constant or modulus of elasticity} \tag{22}$$

Although no stress acts transversely to the axial direction, there will nevertheless be dimensional changes in that direction such that as a bar extends axially, it contracts transversely. The transverse strains ε_2 are related to the axial strains ε_1 by Poisson's ratio ν such that

$$\nu = -\frac{\varepsilon_2}{\varepsilon_1} \tag{23}$$

4

where the negative sign means that the transverse strain will be of the opposite sign to the axial strain. The modulus of elasticity and Poisson's ratio are two important parameters used to describe the material in the analysis of contacting solids.

As the stresses increase within the material, elastic behavior is replaced by plastic flow, in which the material is permanently deformed. The stress state at which the transition from elastic to plastic behavior occurs, known as the yield stress, has a definite value for a given material at a given temperature. In these lectures elastic behavior alone is considered.

When two elastic solids are brought together under a load, a contact area develops, the shape and size of which depend on the applied load, the elastic properties of the materials, and the curvatures of the surfaces. When the two solids shown in figure 2 have a normal load applied to them, the shape of the contact area is elliptical, with a being the semimajor and b the semiminor axis. It has been common to refer to elliptical contacts as point contacts, but since these lectures deal mainly with loaded contacts, the term elliptical contact is adopted. For the special case where $r_{ax} = r_{ay}$ and $r_{bx} = r_{by}$, the resulting contact is a circle rather than an ellipse. Where r_{ay} and r_{by} are both infinite, the initial line contact develops into a rectangle when load is applied.

Figure 5 shows the contact ellipses obtained with either a radial or a thrust load for the ball – inner-race and ball – outer-race contacts in a ball bearing. These lectures are concerned with the conjunctions between solids with contact areas ranging from circular to rectangular. Inasmuch as the size and shape of these contact areas are highly significant to the successful operation of machine elements, it is important to understand their characteristics.

Hertz (1881) considered the stresses and deformations in two perfectly smooth, ellipsoidal, contacting elastic solids much like those shown in figure 2. His application of the classical theory of elasticity to this problem forms the basis of stress calculation for machine elements such as ball and roller bearings, gears, seals, and cams. The following assumptions were made by Hertz (1881):

(1) The materials are homogeneous and the yield stress is not exceeded.
(2) No tangential forces are induced between the solids.
(3) Contact is limited to a small portion of the surface, such that the dimensions of the contact region are small compared with the radii of the ellipsoids.
(4) The solids are at rest and in equilibrium (steady state).

Making use of these assumptions, Hertz (1881) was able to obtain the following expression for the pressure within the ellipsoidal contact shown in figure 6.

$$p = p_{max} \left[1 - \left(\frac{x}{b}\right)^2 - \left(\frac{y}{a}\right)^2 \right]^{1/2} \tag{24}$$

If the pressure is integrated over the contact area, it is found that

$$p_{max} = \frac{3F}{2\pi ab} \tag{25}$$

Equation (24) determines the distribution of pressure or compressive stress on the common interface; it is clearly a maximum at the center of the contact and decreases to zero at the periphery.

5

The ellipticity parameter k can be written in terms of the semimajor and semiminor axes of the contact ellipse as

$$k = \frac{a}{b} \qquad (26)$$

Harris (1966) has shown that the ellipticity parameter can be written as a transcendental equation relating the curvature difference (9) and the elliptic integrals of the first $\mathscr{F}$ and second $\mathscr{E}$ kinds as

$$k = \frac{2\mathscr{F} - \mathscr{E}(1 + \Gamma)}{\mathscr{E}(1 - \Gamma)}^{1/2} \qquad (27)$$

where

$$\mathscr{F} = \int_0^{\pi/2} \left[1 - \left(1 - \frac{1}{k^2} \right) \sin^2\phi \right]^{-1/2} d\phi \qquad (28)$$

$$\mathscr{E} = \int_0^{\pi/2} \left[1 - \left(1 - \frac{1}{k^2} \right) \sin^2\phi \right]^{1/2} d\phi \qquad (29)$$

A one-point iteration method that was adopted by Hamrock and Anderson (1973) can be used to obtain the ellipticity parameter, where

$$k_{n+1} = k_n \qquad (30)$$

The iteration process is normally continued until k_{n+1} differs from k_n by less than 1×10^{-7}. Note that the ellipticity parameter is a function of the radii of curvature of the solids only:

$$k = f(r_{ax}, r_{bx}, r_{ay}, r_{by}) \qquad (31)$$

That is, as the load increases, the semimajor and semiminor axes of the contact ellipse increase proportionately to each other, so the ellipticity parameter remains constant.

Figure 7 shows the ellipticity parameter and the elliptic integrals of the first and second kinds for a range of the curvature ratio R_y/R_x usually encountered in concentrated contacts.

When the ellipicity parameter k, the normal applied load F, Poisson's ratio ν, and the modulus of elasticity E of the contacting solids are known, the semimajor and semiminor axes of the contact ellipse and the maximum deformation at the center of the contact can be written from the analysis of Hertz (1881) as

$$a = \left(\frac{6k^2 \mathscr{E} FR}{\pi E'} \right)^{1/3} \qquad (32)$$

6

$$b = \left(\frac{6\delta FR}{\pi kE'}\right)^{1/3} \tag{33}$$

$$\delta = \mathscr{S}\left[\left(\frac{9}{2\delta R}\right)\left(\frac{F}{\pi kE'}\right)^2\right]^{1/3} \tag{34}$$

where

$$E' = \frac{2}{\dfrac{1 - \nu_a^2}{E_a} + \dfrac{1 - \nu_b^2}{E_b}} \tag{35}$$

In these equations a and b are proportional to $F^{1/3}$ and δ is proportional to $F^{2/3}$.

SUBSURFACE STRESSES

Fatigue cracks usually start at a certain depth below the surface in planes parallel to the direction of rolling. Because of this, special attention must be given to the shear stress amplitude occurring in this plane. Furthermore a maximum shear stress is reached at a certain depth below the surface. The analysis used by Lundberg and Palmgren (1947) will be used to define this stress.

The stresses are referred to a rectangular coordinate system with its origin at the center of the contact, its z-axis coinciding with the interior normal of the body considered, its x-axis in the direction of rolling, and its y-axis in the direction perpendicular to the rolling direction. In the analysis that follows it is assumed that $y = 0$.

From Lundberg and Palmgren (1947) the following equations can be written:

$$\tau_{zx} = \frac{3F}{2\pi}\frac{\cos^2\phi \sin\phi \sin\gamma}{(a^2\tan^2\gamma + b^2\cos^2\phi)} \tag{36}$$

$$x = \sqrt{b^2 + a^2\tan^2\gamma}\,\sin\phi \tag{37}$$

$$z = a \tan\gamma \cos\phi \tag{38}$$

The maximum shear stress amplitude is defined as

$$\tau_0 = \left|\tau_{zx}\right|_{max}$$

The amplitude of the shear stress τ_0 is obtained from

7

$$\frac{\partial \tau_{zx}}{\partial \phi} = 0$$

$$\frac{\partial \tau_{zx}}{\partial \gamma} = 0$$

For the point of maximum shear stress

$$\tan^2 \phi = t_a \tag{39}$$

$$\tan^2 \gamma = t_a - 1 \tag{40}$$

$$\frac{1}{k} = \sqrt{\left(t_a^2 - 1\right)\left(2t_a - 1\right)} \tag{41}$$

The position of the maximum point is determined by

$$z = z_0 = \zeta^* b \tag{42}$$

$$z = \pm_n^* b \tag{43}$$

where

$$\zeta^* = \frac{1}{(t_a + 1)\sqrt{2t_a - 1}} \tag{44}$$

$$n^* = \frac{t_a}{t_a + 1} \sqrt{\frac{2t_a + 1}{2t_a - 1}} \tag{45}$$

Furthermore the magnitude of the maximum shear stress is given by

$$\tau_0 = \left(\frac{3F}{2\pi ab}\right) \frac{\sqrt{2t_a - 1}}{2t_a(t_a + 1)} \tag{46}$$

SIMPLIFIED SOLUTION FOR STRESSES AND DEFORMATIONS

The classical Hertzian solution presented in the previous section requires the calculation of the ellipticity parameter k and the complete elliptic integrals of the first and second kinds $\mathcal{F}$ and $\mathcal{E}$. This entails finding a solution to a transcendental equation relating k, $\mathcal{F}$, and $\mathcal{E}$ to the geometry of the contacting solids, as expressed in (27). This is usu-

ally accomplished by some iterative numerical procedure, as described by Hamrock and Anderson (1973), or with the aid of charts, as shown by Jones (1946).

Brewe and Hamrock (1977) used a linear regression by the method of least squares to obtain simplified equations for k, $\mathscr{F}$, and $\mathscr{E}$. That is, for given sets of pairs of data, $\{[k_j, (R_y/R_x)_j], j = 1, 2, \ldots, n\}$, a power fit using a linear regression by the method of least squares resulted in the following equation:

$$\bar{k} = 1.0339 \left(\frac{R_y}{R_x}\right)^{0.6360} \tag{47}$$

The asymptotic behavior of $\mathscr{E}$ and $\mathscr{F}$ was suggestive of the functional dependence that $\mathscr{E}$ and $\mathscr{F}$ might exhibit. As a result a logarithmic and an inverse curve fit were tried for $\mathscr{E}$ and $\mathscr{F}$, respectively. The following expressions from Brewe and Hamrock (1977) provide an excellent approximation to the relationships between $\mathscr{E}$, $\mathscr{F}$ and R_y/R_x:

$$\bar{\mathscr{E}} = 1.0003 + \frac{0.5968}{R_y/R_x} \tag{48}$$

$$\bar{\mathscr{F}} = 1.5277 + 0.6023 \ln (R_y/R_x) \tag{49}$$

Values of $\bar{k}$, $\bar{\mathscr{E}}$, and $\bar{\mathscr{F}}$ are presented in table 1 and compared with the Hamrock and Anderson (1973) numerically determined values of k, $\mathscr{E}$, and $\mathscr{F}$. The agreement is good.

Using these simplified expressions for $\bar{k}$, $\bar{\mathscr{E}}$, and $\bar{\mathscr{F}}$ and equation (34) gives the deformation at the center of the contact

$$\bar{\delta} = \left(\frac{F}{K}\right)^{2/3} \tag{50}$$

where

$$K = \pi \bar{k} E' \left(\frac{R\bar{\mathscr{E}}}{4.5\bar{\mathscr{F}}^3}\right)^{1/2} \tag{51}$$

Note that the load-deflection constant K is a function of the geometry and the material properties.

The results of comparing $\bar{\delta}$ with δ are also shown in table 1. The agreement is again quite good. Therefore the deformation at the center of the contact can be obtained directly from (47) to (51). This valuable approximation eliminates the need to use curve fitting, charts, or numerical methods.

Figure 8 shows three different degrees of ball-contact conformity: a ball on a ball, a ball on a plane, and a ball - outer-ring contact. Table 2 uses this figure to show how the degree of conformity affects the contact parameters. The table shows that k is not exactly equal to unity for the ball-on-ball and ball-on-plane situations because of the approximation represented by equation (47). The diameter of the balls is the same throughout, and the material of the solids is steel. The ball - outer-ring

9

contact is representative of a 209 radial ball bearing. A 4.45-N (1-lbf)
normal load has been considered for each situation. The maximum pressure
decreases significantly as the curvature of the mating surface approaches
that of the ball. Table 2 shows that the curvature of the mating surfaces
is very important in relation to the magnitude of the maximum pressure or
surface stress produced. A ball and ring of high conformity are thus
desirable from the standpoint of minimizing the stress.

Table 2 also shows that the area of the contact πab increases with
the conformity of the contacting solids. Although this effect minimizes
contact stresses, it can have an undesirable effect on the force of friction
since friction force increases as the contact area, and hence the area of
the sheared lubricant, increase in a bearing operating under elastohydro-
dynamic conditions. The curvatures of the bearing races are therefore gen-
erally a compromise that takes into consideration the stress, load capacity,
and friction characteristics of the bearing.

In equations (42) to (46) the location and magnitude of the maximum sub-
surface shear stress are written as functions of t_a, an auxiliary parame-
ter. Furthermore in equation (41) the ellipticity parameter is written as a
function of t_a. The range for $1/k$ is $0 < 1/k < 1$, and the correspond-
ing range for t_a is $0 \le t_a \le (1 + \sqrt{17})/4$. A linear regression by the
method of least squares was used to obtain a simplified formula for t_a
in terms of k, the ellipticity parameter. That is, for given sets of pairs
of data $\{[(1 - t_a)_j, (1/k)_j], j = 1, 2, \ldots, n\}$, a power fit using a
linear regression by the method of least squares resulted in the following
equation:

$$t_a - 1 = 0.3044 \left(\frac{1}{k}\right)^{1.8559} \tag{52}$$

The agreement between this approximate equation and the exact solution is
within ±2 percent. Using equation (52) greatly simplifies finding the val-
ues for the location and magnitude of the maximum subsurface shear stress
expressed in equations (42) to (46).

CONCLUDING REMARKS

An assorted group of topics has been presented dealing with conformal
and nonconformal surfaces, curvature sum and difference, and surface and
subsurface stresses in elliptical contacts. Load-deflection relationships
have been developed for any type of contact. The deformation within the
contact is a function, among other things, of the ellipticity parameter and
elliptic integrals of the first and second kinds. Simplified expressions
have been written that allow deformation to be calculated quickly and, gen-
erally, with adequate accuracy. A simplified expression was also developed
that enables the location and magnitude of the maximum subsurface shear
stress to be written directly without relying on an iterative procedure.

APPENDIX - SYMBOLS

a	semimajor axis of contact ellipse, m
b	semiminor axis of contact ellipse, m
d	ball diameter, m
d_e	pitch diameter, m
E	modulus of elasticity, N/m^2
E'	effective modulus of elasticity, $2 \left/ \left[\dfrac{1 - v_a^2}{E_a} + \dfrac{1 - v_b^2}{E_b} \right] \right.$, N/m^2
$\mathcal{E}$	elliptic integral of second kind with modulus $(1 - 1/k^2)^{1/2}$
F	normal applied load, N
$\mathcal{F}$	elliptic integral of first kind with modulus $(1 - 1/k^2)^{1/2}$
K	load-deflection constant defined in eq. (51)
k	ellipticity parameter, a/b
p	pressure, N/m^2
p_{max}	maximum pressure within contact, $3F/2\pi ab$, N/m^2
R	curvature sum, m
r	race curvature radius, m
S	geometrical separation of ellipsoidal solids, m
t_a	auxiliary parameter
x,y,z	coordinate system
β	contact angle
Γ	curvature difference
δ	elastic deformation, m
ϵ_1	strain in axial direction
ϵ_2	strain in transverse direction
v	Poisson's ratio
σ_1	stress in axial direction, N/m^2
τ	shear stress, N/m^2
τ_0	maximum subsurface stress, N/m^2

Subscripts:

a	solid a
b	solid b
i	inner race
o	outer race
x,y,z	coordinate system

Superscript:

( )	approximate

11

REFERENCES

Brewe, D. E.; and Hamrock, B. J.: Simplified Solution for Elliptical-Contact Deformation Between Two Elastic Solids. J. Lubr. Technol., vol. 99, no. 4, pp. 485-487, 1977.

Hamrock, B. J; and Anderson, W. J.: Analysis of an Arched Outer-Race Ball Bearing Considering Centrifugal Forces. J. Lubr. Technol., vol. 95, no. 3, pp. 265-276, 1973.

Harris, T. A.: Rolling Bearing Analysis, John Wiley & Sons, New York, 1966.

Hertz, H.: The Contact of Elastic Solids. J. Reine Angew. Math., vol. 92, 1881.

Jones, A. B.: Analysis of Stresses and Deflections. New Departure Engineering Data. General Motors Corp., Bristol, Conn., 1946.

Lundberg, G.; and Palmgren, A.: Dynamic Capacity of Rolling Bearings. Acta Polytech., Mech. Eng. Ser., vol. 1, no. 3, 1947.

TABLE 1. - COMPARISON OF APPROXIMATE AND EXACT FORMULAS

Radius Ratio, R_y/R_x	Ellipticity			Elliptic Integrals						Deformation at Center of Contact		
	k	$\bar{k}$	Percent Error	Second kind			First kind			Numerical, δ	From Curve Fit Equation, $\bar{\delta}$	Percent Error
				$\mathscr{E}$	$\bar{\mathscr{E}}$	Percent Error	$\mathscr{F}$	$\bar{\mathscr{F}}$	Percent Error			
1.000	1.00	1.03	3.00	1.57	1.60	1.91	1.57	1.53	-2.55	1.230×10^{-4}	1.168×10^{-4}	-5.04
2.820	1.99	2.00	.50	1.21	1.21	0	2.15	2.15	0	1.020	1.017	-.29
5.314	3.01	3.00	-.33	1.11	1.11		2.53	2.53	0	.897	.899	.22
8.330	4.01	4.00	-.25	1.07	1.07		2.80	2.80	0	.814	.816	.25
11.805	4.99	5.00	.20	1.05	1.05		3.02	3.01	-.29	.756	.752	-.53
15.697	5.97	6.00	.50	1.04	1.04		3.19	3.18	-.25	.706	.701	-.71
19.971	6.92	7.00	1.16	1.03	1.03		3.33	3.33	0	.667	.662	-.75
24.605	7.87	8.00	1.65	1.02	1.02		3.46	3.45	-.24	.636	.628	-1.26
29.576	8.80	9.00	2.27	1.02	1.02		3.57	3.56	-.22	.608	.598	-1.64
34.869	9.72	10.00	2.88	1.02	1.02		3.67	3.66	-.25	.584	.571	-2.23

TABLE 2. - EFFECT OF DEGREE OF CONFORMITY

CONTACT PARAMETERS

[For all three cases, $E' = 2.28\times10^{11}$ N/m^2 (steel on steel), $F = 4.45$ N, and $r_{ax} = r_{ay} = 6.35$ mm. For the ball - outer ring contact, $d_e = 65$ mm, $\beta = 0°$, $f_o = 0.52$ (assume 209 radial ball bearing).]

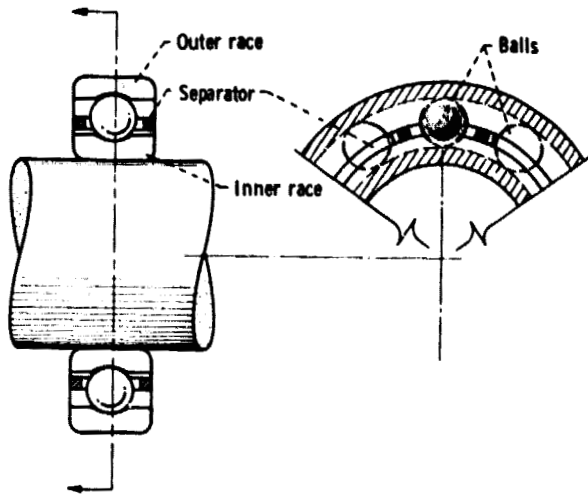| Contact Parameters	Ball on Ball	Ball on Plane	Ball - Outer Ring Contact
r_{bx}	6.35 mm	∞	-38.9 mm
r_{by}	6.35 mm	∞	-6.60 mm
R	1.59 mm	3.18 mm	7.26 mm
R_y/R_x	1	1	22.1
$\bar{k}$	1.02	1.03	7.330
$\bar{\mathscr{E}}$	1.60	1.60	1.03
$\bar{\mathscr{F}}$	1.53	1.53	3.38
$\bar{a}$	0.0465 mm	0.0586 mm	0.247 mm
$\bar{b}$	0.0451 mm	0.0569 mm	0.0336 mm
πab	0.659×10^{-2} mm^2	1.04×10^{-2} mm^2	2.60×10^{-2} mm^2
$\bar{\delta}$	6.31×10^{-4} mm	4.87×10^{-4} mm	2.56×10^{-4} mm
$\bar{p}_{max}$	1.01×10^{9} N/m^2	0.657×10^{9} N/m^2	0.256×10^{9} N/m^2

Figure 1. - Ball bearing components. Example of nonconformal surfaces.
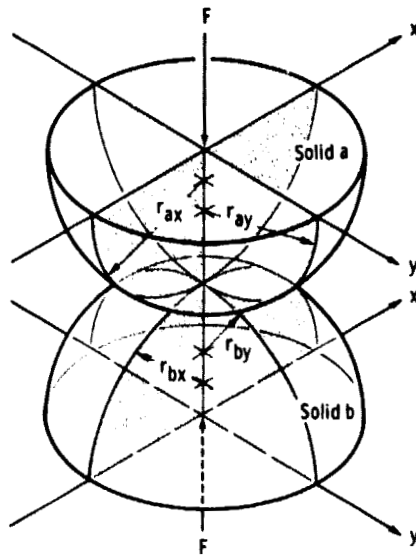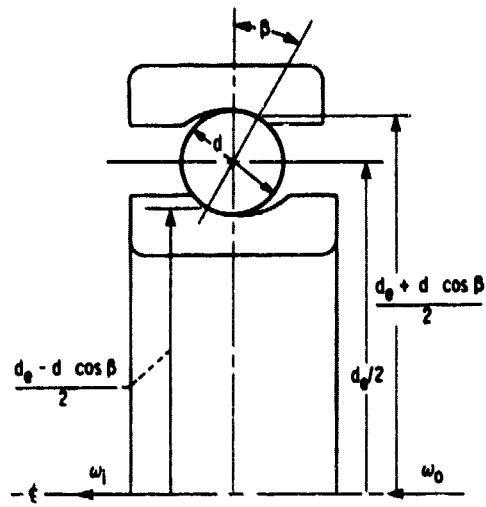

Figure 2. - Geometry of contacting elastic solids.

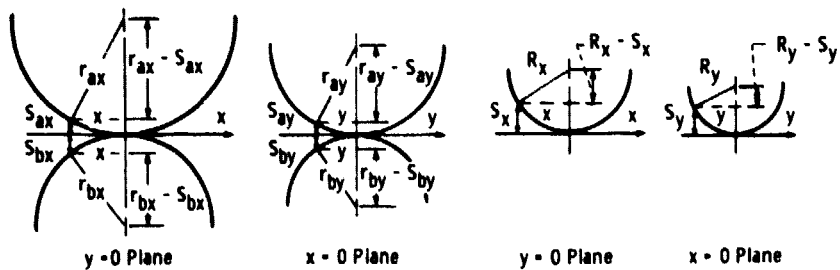Figure 3. - Cross section of ball bearing.

y - 0 Plane   x - 0 Plane   y - 0 Plane   x - 0 Plane

(a) Two different ellipsoidal solids.   (b) Equivalent ellipsoidal solid near a plane.
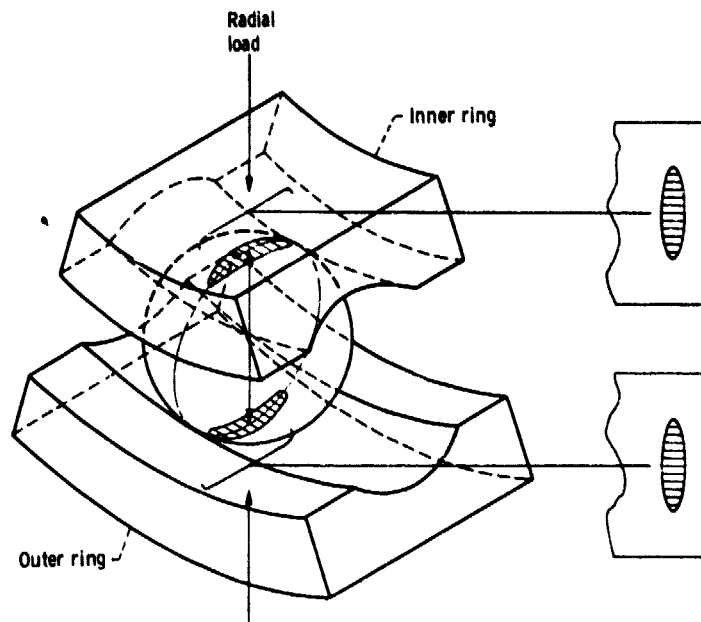
Figure 4. - Equivalent ellipsoidal solids.
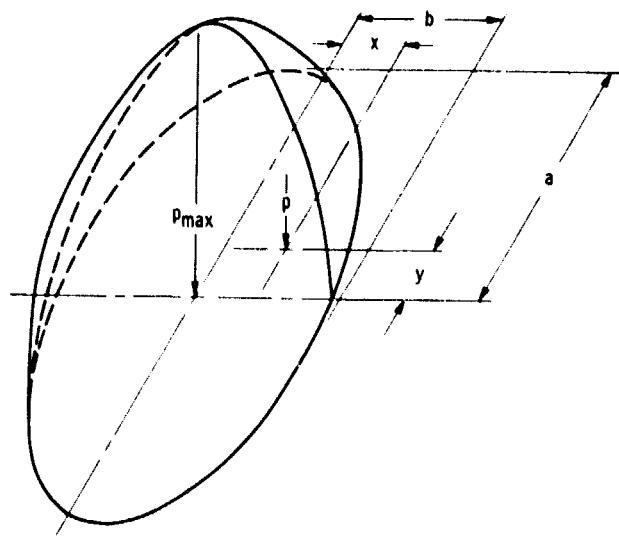
Figure 5. - Contact areas in a ball bearing.

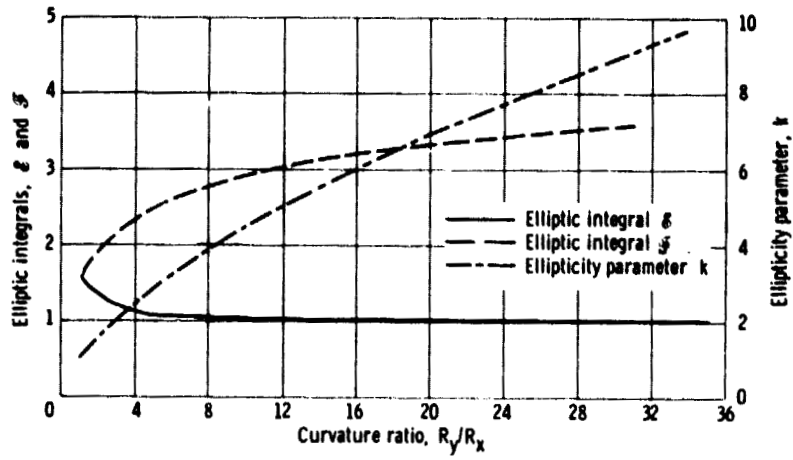Figure 6. - Pressure distribution in an ellipsoidal contact.

Figure 7. - Ellipticity parameter and elliptic integrals of first and second kinds as a function of curvature ratio.
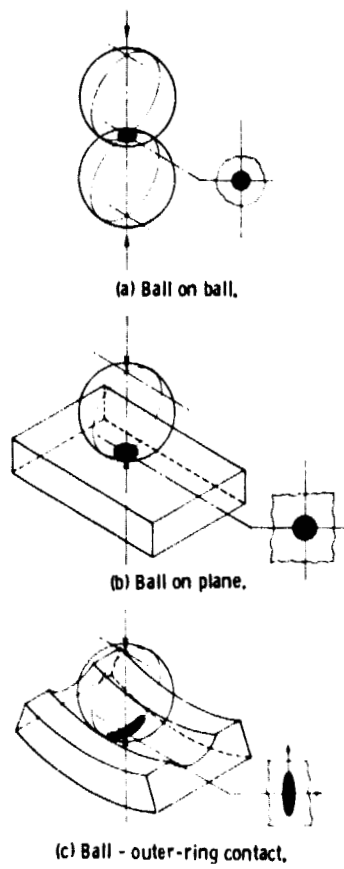

(a) Ball on ball.

(b) Ball on plane.

(c) Ball - outer-ring contact.

Figure 8. - Three degrees of conformity.